Kavita[1,2], Veena Sharma[1], Gian C. Rana[3]*

ELECTROCONVECTION IN ROTATING PULSATING THROUGHFLOW NANOFLUID SATURATED BY POROUS LAYER WITH REALISTIC MODEL

ELEKTROKONVEKCIJA U ROTIRAJUĆEM PULSIRAJUĆEM STRUJANJU NANOFLUIDA SA ZASIĆENIM POROZNIM SLOJEM U REALNOM MODELU

Originalni naučni rad / Original scientific paper
UDK /UDC:

Rad primljen / Paper received: 27.01.2022

Adresa autora / Author's address:
[1)] Depart. of Mathematics and Statistics, Himachal Pradesh University, Shimla-5, India, *email: pc.vs441@gmail.com
[2)] Department of Mathematics, Govt. Degree College Mandi, Himachal Pradesh, India
[3)] Department of Mathematics, NSCBM Govt. College, Hamirpur, Himachal Pradesh, India,
email: drgcrana15@gmail.com

Keywords
- nanofluid
- pulsating throughflow
- electric field
- rotation
- porous medium

Abstract

Linear stability convection in a nanofluid layer of pulsating throughflow and rotating about the vertical saturating a porous layer heated at the lower surface with the inclusion of an external vertical AC electric field is developed for realistic boundary conditions, in which volume fraction flux of nanoparticles is taken to be zero on the isothermal boundaries. The basic profile for temperature gets altered for this flow and the volumetric fraction of nanoparticle vary from linear to nonlinear with layer height, which marks the stability expressively. The exact solutions of the characteristic equation for both stress-free bounding surfaces are obtained analytically and the expressions of the thermal Rayleigh number for onset of both oscillatory and stationary modes are derived in terms of a variety of non-dimensional involved parameters. The pulsating throughflow, rotation and Lewis number are found to decrease size of the cellular stationary modes, whereas these are increased with rise in modified diffusivity ratio, the electric Rayleigh number, the medium porosity and Rayleigh number of nanoparticle concentration. The occurrence of oscillatory mode is ruled out for the realistic boundary conditions. The numerically computed values of the thermal Rayleigh number for stationary modes are plotted.

Ključne reči
- nanofluid
- pulsirajuće strujanje
- električno polje
- rotacija
- porozna sredina

Izvod

Linearna stabilna konvekcija u nanofluidnom sloju pulsirajućeg strujanja i rotacije oko vertikalnog zasićenog poroznog sloja koji se zagreva na donjoj površini i sa dodatkom spoljašnjeg vertikalnog električnog polja naizmenične struje, je razvijena u realnim graničnim uslovima, gde je udeo zapreminskog fluksa nanočestica jednak nuli na izotermskim granicama. Osnovni temperaturski profil se menja u ovom strujanju i zapreminski udeo nanočestica se menja od linearnog ka nelinearnom po debljini sloja, čime se izrazito uočava stabilnost. Tačna rešenja karakteristične jednačine za obe slobodne granične površine bez napona su dobijena analitički, a izrazi za termički Rejlejev broj pri nastupanju oscilatornih i stacionarnih režima su izvedeni sa skupom bezdimenzionih parametara. Pulsirajuće strujanje, rotacija i Luisov broj opadaju sa veličinom posude u stacionarnom režimu, dok s druge strane rastu sa porastom modifikovanog koeficijenta difuzije, električnog Rejlejevog broja, poroznosti sredine i Rejlejevog broja koncentracije nanočestica. Odbacuje se oscilatorni režim u realnim graničnim uslovima. Dati su dijagrami numerički određenih veličina termičkog Rejlejevog broja za stacionarne režime.

INTRODUCTION

Electro-hydrodynamics (EHD) is the study of motion of electrically charged particles or molecules in fluids due to the inclusion of external electric field and finds crucial role in dielectric fluids with low electric conductivity. Distilled water, most of organic substances and transformer oil are a few examples of dielectric fluids. Electroconvection in dielectric liquids has remained the focus of research over the past couple of decades after the experimental work by Gross and Porter /1/. They experienced very interesting result that the electric field established the convective pattern exactly similar to that of the familiar Bénard cells in natural convection. The impact of forces due to electrophoresis on the Bénard convection has been studied by Turnbull /2/ and the validity of PES (principle of exchange of stabilities) was proved over a certain set of boundary conditions.

The pulsating throughflows have achieved great potential for the last 3-4 decades due to their diverse applications in industrial as well as biological processes such as respiratory and circulatory systems, reciprocating pumps, vascular diseases, pulse combustors and IC engines. Pulse is the one of the active techniques to create a shock in the fluid motion to increase the heat transfer, which is the best way to increase the efficiency of heat exchangers. Wang /3/ analysed this flow in a porous medium. Ishino et al. /4/ investigated the impact of pulsating on the fluid flow and heat transfer. They analysed the effect of throughflow in fluid and transfer of heat with the inclusion of three pulsating parameters i.e., the frequency, the amplitude, and the mean velocity assuming boundary conditions of wall temperature constant. Nanofluids are the fluids formed by adding nanoparticles having size 10-50 nm in traditional fluids first coined by Choi /5/. These base fluids may be of aqueous or non-aqueous nature and regular nano size particles are like oxides, nitrides, carbides of metals, carbon nanotubes etc.

Nanofluids are now considered of great potential in the present era to enhance the heat transfer, the characteristics of which are influenced primarily by specific heat, thermal conductivity, viscosity and density, size of particles, pH and zeta potential /6-9/. These fluids are usable in nano- composites, oil drilling, electronic cooling, bio medicines and nano structure fabrication transportation. Many researchers studied different properties of nanofluids along with their application, scenario of applications both experimentally and numerically /10-13/.

Buongiorno /14/ formulated a mathematical model to capture the base fluid/nanoparticle slip by considering nanofluid as a mixture of two components and showed that the prior mechanisms accounting for the relative slip velocity between base fluid and nanoparticles are thermophoresis and Brownian motion. Agarwal and Kuznetsov /15/ studied the onset of natural convection for flow in nanofluid saturating a porous medium by employing Darcy model. Rayleigh-Bénard convection in nanofluids was examined by Dhananjay et al. /16/. Xu and Xing /17/ numerically studied the flow and thermal performance of natural convection of a nanofluid flowing in a porous medium cavity by using the proposed LB model and found that the highly conductive porous foam and nanofluid will obviously improve natural convection's thermal performance, and its combination show a great potentiality for applications requiring a lot of heat flux.

Coriolis forces are induced on spreading a nanofluid under the acceleration due to gravity and rotation vector normal to flow motions, which tends to show opposite influence on the spreading of flow. When viscous dissipator boundaries intersect isopotential surface, an equilibrium of geotropic state is reached, implying thereby a balance between Coriolis and buoyancy forces. Significance of rotation on the onset of thermal instability in porous medium have been established by several researchers /18-23/. Shivakumara and Nagashree /24/ studied the impact of electrothermoconvection in a rotating Brinkman porous layer. Yadav et al. /25/ examined the thermal instability of rotating nanofluid layers using a physically more realistic boundary condition on the nanoparticle volumetric fraction and they have found a stabilizing effect of rotation on the system. Bakar et al. /26/ investigated the boundary layer flow and heat transfer in rotating nanofluid across a stretching sheet using the Buongiorno model and thermophysical properties of nanoliquids. Yadav /27/ has analysed numerically the importance of rotation and varying acceleration due to gravity on the occurrence of convection in nanofluid saturated porous layer for both the cases of linear and parabolic variations in the gravity field.

Several applications of electric field in dielectric fluids with low electric conductivity under variety of mechanisms are reviewed by Zhakin /28/. Some of these include heat exchange enhancement by EHD pumping, EHD- based devices used in aerospace industry to control vibrations and noise, formation of semiconductor by doping. Yadav et al. /29/ have given attention to the analysis of effect of electrothermal instability in the presence of nanoparticles in nanofluid layer. Chand and Rana /30/ investigated the impact of vertical AC electric field on the thermal convection in a rotating nanofluids by using the generalized Darcy-Brinkman model for porous media. Sharma et al. /31/ have investigated thermal convection of dielectric nanofluids in presence AC electric field. They observed the occurrence of oscillatory motion for case of bottom-heavy as well as top-heavy distributions of nanoparticles. Recently, Rana et al. /32-35/ studied the effect of vertical AC electric field and rotation on the onset of thermal convection in a nanofluid layer for free-free boundaries whereas Gautam et al. /36/ studied the effect of vertical AC electric field on the onset of thermal convection in a nanofluid layer for free-free, rigid-free and rigid-rigid boundaries and found that the vertical AC electric field has destabilising influence, and rotation has stabilising influence on the system.

The pulsating flow increases flow of fluid which depend on the nanofluids concentration and flow rate. Yadav /37/ studied the influence of pulsating throughflow of electrohydrodynamic convection in dielectric nanofluids saturated porous medium and found that amplitude of throughflow on varying frequency increases the stability of the system. The effect of pulsating throughflow on nanofluid thermal convection and heat transfer has been studied by many researchers /38-40/. Yadav /41/ investigated the combined influence of pulsing throughflow and magnetic field on the onset of convective instability in a nanofluid layer bounded in a Hele-Shaw cell. Recently, simultaneous effect of rotation and pulsating throughflow on the development of longitudinal convective rolls in a porous media saturated by nanofluid is highlighted using the frozen profile method by Yadav /42/ and Yadav et al. /43/. They demonstrated that pulsing throughflow in both directions has a stabilizing impact. Oscillations of throughflow with higher amplitude are also found to stabilize a system to a large extent, which depends on the frequency. Recently, Vijayalakshmi et al. /44/ studied the hydromagnetic pulsating flow of nanofluid between two parallel walls with porous medium whereas Somasundaram and Reddy /45/ studied pulsating flow of electrically conducting couple stress nanofluid in a channel with Ohmic dissipation and thermal radiation and found that velocity of nanofluid increases with an increment in frequency parameter.

Motivated by above studies, an attempt has been made to examine the onset of electroconvection in a rotating nanofluid with a vertical angular velocity, an AC electric field and pulsating throughflow in a porous medium by employing Darcy law of resistance forces, theoretically and analytically. The stress-free boundary conditions with zero volume fraction of nanoparticles are taken. This is an extension of the work of Yadav /42/. To the best knowledge of the authors this work has not been carried out yet.

MATHEMATICAL FORMULATION

An incompressible nanofluid with infinite extending electrically conducting horizontal layer with thickness d between two parallel xy-planes is considered, which is heated from below in an isotropic porous medium of homogeneous medium porosity and medium permeability with temperature T_0 at $z = 0$ toward lower plane and T_1 at $z = d$ toward upper plane with angular velocity $\vec{\Omega} = (0, 0, \Omega)$ as shown in Fig. 1. Both upper and lower boundaries are kept at constant temperature, respectively, ($T_1 < T_0$). Volumetric fraction flux of nanoparticles, J_z vanishes on both upper and lower plates. A vertical acceleration due to gravity force $\vec{g}$ (0, 0, $-g$) acts across the nanofluid and a uniform vertical external AC electric field is applied across the nanofluid layer. An electric circuit is maintained at lower bounding surface, whilst potentials with root mean square value φ is considered at upper bounding surface.

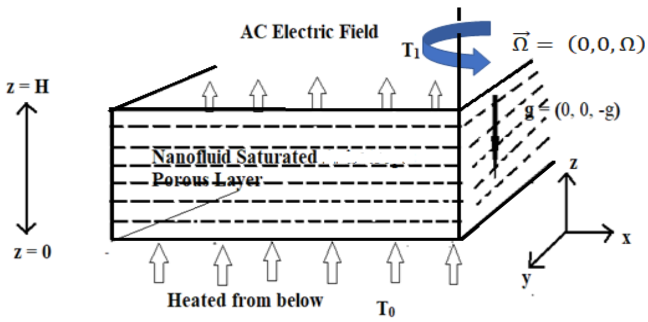

Figure 1. Physical configuration of the problem.

The equations of conservation of mass, momentum and energy using Boussinesq approximation for incompressible rotating nanofluid in pulsating throughflow saturated porous medium are /14, 15, 20, 36, 45/

$$\nabla.\overrightarrow{q_n} = 0\,, \tag{1}$$

$$0 = -\nabla p_n + \overrightarrow{f_e} + \left[\phi_n \rho_P + (1-\phi_n)\rho_f\{1-\beta(T-T_0)\}\right]\vec{g} - $$
$$-\frac{\mu}{k_1}\overrightarrow{q_n} + \frac{2\rho_0}{\varepsilon_n}(\overrightarrow{q_n}\times\vec{\Omega})\,, \tag{2}$$

$$\frac{\partial \phi_n}{\partial t} + \frac{1}{\varepsilon_n}(\vec{q}_n.\nabla)\phi_n = \nabla.\left[D_B\nabla\phi_n + \frac{D_T}{T_0}\nabla T\right], \tag{3}$$

$$(\rho s)_m \frac{\partial T}{\partial t} + (\rho s)_f(\overrightarrow{q_n}.\nabla)T = \nabla.(k_m.\nabla T) +$$
$$+\varepsilon_n(\rho s)_P\nabla T.\left[D_B\nabla\phi_n + \frac{D_T}{T_0}\nabla T\right], \tag{4}$$

where: $\overrightarrow{q_n}$ (u, v, w), k_1, ρ_P, ϕ_n, k_m, ρ_f, μ, ε_n, β, D_B, D_T, S represent Darcy velocity vector, medium permeability, density, volume fraction for nanoparticles, effective thermal conductivity, base fluids density, fluid dynamic viscosity, medium porosity, coefficient of thermal expansion, Brownian diffusion coefficient, thermophoretic diffusion coefficient, specific heat at constant pressure, respectively.

The electrical origin force /32/ $\overrightarrow{f_e}$ due to the presence of electric field is

$$\overrightarrow{f_e} = \rho_e\overrightarrow{E_n} - \frac{1}{2}\overrightarrow{E_n}^2\nabla\gamma_n + \frac{1}{2}\nabla\left(\rho\frac{\partial\gamma_n}{\partial\rho}\overrightarrow{E_n}^2\right). \tag{5}$$

Here, ρ_e and $\overrightarrow{E_n}$ represent density of charged particle and electric field, respectively. On right hand side of Eq.(5) first two terms are due to the presence of free charge particle (also known as coulomb force) and gradient of dielectric constant, and the last term is electrostriction term which is added with pressure p_n in Eq.(2), without affecting the incompressibility of fluid. Thus, the modified pressure is given as:

$$\vec{P} = p_n - \frac{1}{2}\nabla\left(\rho\frac{\partial\gamma_n}{\partial t}\overrightarrow{E_n}^2\right). \tag{6}$$

Dielectric constant, γ_n and nanofluid density, ρ are given by

$$\gamma_n = \gamma_0\left[1-e(T-T_0)\right], \quad \rho = \rho_0\left[1-\alpha(T-T_0)\right]. \tag{7}$$

Here, e is the coefficient of dielectric constant, and α is the coefficient of volume expansion.

Assuming negligible density, /35/ are

$$\nabla.(\gamma_n\overrightarrow{E_n}) = 0\,, \quad \nabla\times\overrightarrow{E_n} = 0\,. \tag{8}$$

Second of Eq.(8), $\overrightarrow{E_n}$ can also be written in terms of electric potential as

$$\overrightarrow{E_n} = -\nabla\varphi\,. \tag{9}$$

Since nanoparticles volume fraction on both the stress-free bounding surfaces with uniform temperature vanish and the bounding surfaces are conducting perfectly. Therefore, Dirichlet boundary conditions of temperature are known as realistic. Thus, the appropriate boundary conditions to be satisfied are

$$w = w_c(1+\tau\cos\omega_1 t_1)\,,\quad T = T_0\,,\quad J_z = 0 \quad \text{at} \quad z = 0 \quad \text{and}$$
$$w = w_c(1+\tau\cos\omega_1 t_1)\,,\quad T = T_1\,,\quad J_z = 0 \quad \text{at} \quad z = d\,, \tag{10}$$

where: $J_z = -\rho_P\left[D_B\frac{\partial\phi_n}{\partial z} + \frac{D_T}{T_1}\frac{\partial T}{\partial z}\right]$ is the flux of nanoparticles volumetric fraction; w, ω_1 and τ represent vertical velocity of nanoparticles, angular frequency vertical velocity of nanoparticle, and amplitude of pulsation, respectively.

Introducing the non-dimensional variables for physical quantities

$$(x_1^*, y_1^*, z_1^*) = \frac{(x,y,z)}{d}\,,\quad \overrightarrow{q_n}^* = \frac{d}{\alpha_m}\overrightarrow{q_n}\,,\quad \vec{t}^* = \frac{\alpha_m}{\varepsilon_n d^2}t\,,$$

$$P^* = \frac{k_1}{\mu\alpha_m}P\,,\quad \phi_n^* = \frac{(\phi_n - \phi_{n_0})}{\phi_{n_0}}\,,\quad T^* = \frac{(T-T_0)}{\Delta T}\,,$$

$$\overrightarrow{E_n}^* = \frac{1}{e\Delta T E_0}\overrightarrow{E_n}\,,\quad \varphi^* = \frac{1}{e\Delta T d E_0}\varphi\,,\quad J_z^* = \frac{d}{\rho_P D_B\phi_{n_0}}J_z\,,$$

$$\gamma_n^* = \frac{1}{\gamma_0}\gamma_n \quad \text{and} \quad \Delta T = T_0 - T_1\,, \tag{11}$$

where: $\alpha_m = \dfrac{k_m}{(\rho c)}$, $\sigma = \dfrac{(\rho s)_m}{(\rho s)}$.

Equations (1)-(4) and (7)-(9) in non-dimensional form after using Eq.(11) become

$$\nabla.\overrightarrow{q_n}=0\,, \tag{12}$$

$$0=-\nabla P+\overrightarrow{q_n}+\sqrt{T_a}\,(v\hat{i}-u\hat{j})+T(R_a-R_e)\hat{e}_z- -\phi_n R_N\hat{e}_z+R_e\frac{\partial\varphi}{\partial z}\,, \tag{13}$$

$$\frac{1}{\sigma}\frac{\partial\phi_n}{\partial t}+\frac{1}{\varepsilon_n}(\overrightarrow{q_n}.\nabla)\phi_n=\frac{1}{L_e}\nabla^2\phi_n+\frac{N_A}{L_e}\nabla^2 T\,, \tag{14}$$

$$\frac{\partial T}{\partial t}+(\overrightarrow{q_n}.\nabla)T=\nabla^2 T+\frac{N_B}{L_e}\left[\nabla\phi_n+N_A\nabla T\right].\nabla T\,, \tag{15}$$

$$\nabla.(\gamma_n\overrightarrow{E_n})=0\,,\quad \nabla\times\overrightarrow{E_n}=0\,,\quad \overrightarrow{E_n}=-\nabla\varphi\,, \tag{16}$$

$$\gamma_n=(1-eT\Delta T)\,, \tag{17}$$

$$J_z=-\left(\frac{\partial\phi_n}{\partial z}+N_A\frac{\partial T}{\partial z}\right). \tag{18}$$

Here, $R_a=\dfrac{dkg\beta\rho_f\Delta T}{\mu\alpha_m}$ is the thermal Darcy-Rayleigh number, $R_N=\dfrac{dk\phi_0(\rho_p-\rho_f)g}{\mu\alpha_m}$ is concentration Darcy-Rayleigh number, $R_e=\dfrac{\gamma_0 e^2E_0^2\beta^2d^2k}{\mu\alpha_m}$ is the AC electric Rayleigh number, $L_e=\dfrac{\alpha_m}{\varepsilon_n D_B}$ is the Lewis number, $N_A=\dfrac{D_T\Delta T}{D_B T_0}$ is the modified diffusivity ratio, $U=\dfrac{dw_c}{\kappa_v}$ the Péclet number, and $\omega=\dfrac{\sigma d^2}{\alpha_m}\omega_1$ the angular frequency, $N_B=\varepsilon_n\dfrac{(\rho s)_P\phi_0}{(\rho s)_f}$ the modified particle density increment, $T_a=\left(\dfrac{2\Omega d^2}{\varepsilon_n\nu}\right)^2$ modified Taylor number are the non-dimensional parameters.

The boundary conditions Eq.(10) become

$$w=U(1+\tau\cos\omega t)\,,\ T=1\,,\ J_z=0\quad\text{at}\quad z=0\quad\text{and}$$

$$w=U(1+\tau\cos\omega t)\,,\ T=0\,,\ J_z=0\quad\text{at}\quad z=1\,. \tag{19}$$

BASIC STATE

Since there is no motion in the fluid flow initially and settling of the suspended nanoparticles in fluid, therefore, basic state solutions are given as

$$\overrightarrow{q_b}=Q_1\hat{k}\,,\ P_b=P(z)\,,\ T_b=T_b(z)=T_0-\beta z\,,$$

$$\gamma_b=\gamma_b(z)=\gamma_0(1+e\alpha z)\,,\ \overrightarrow{E_b}=E_b(z)\hat{k}\,, \tag{20}$$

$$\phi_b=\phi_b(z)\,,\ \varphi_b=\varphi_b(z)=-\log\frac{1+e\Delta Tz}{(e\Delta T)^2}\,, \tag{21}$$

where: $Q_1=U(1+\tau\cos\omega t)$.

The solutions appropriate to basic state Eq.(20) are

$$T_b=\frac{e^{Q_1}-e^{Q_1 z}}{e^{Q_1}-1}\,, \tag{22}$$

$$\phi_b=\frac{N_A}{(Q_1-Q_2)}\left[\frac{\left(e^{Q_1 z}-1\right)}{\left(e^{Q_1}-1\right)}Q_1-\frac{\left(e^{Q_2 z}-1\right)}{\left(e^{Q_2}-1\right)}Q_2\right]+\phi_0\,, \tag{23}$$

$$E_b=\frac{1}{e\Delta T(1+e\Delta Tz)}\,, \tag{24}$$

$$J_{zb}=0\,, \tag{25}$$

where, $Q_2=\dfrac{Q_1L_e}{\varepsilon_n}$, $E_0=-\dfrac{e\Delta T\varphi_1}{\log(1+e\Delta T)}$, $\phi_0=\dfrac{\phi_b(0)-\phi_{n_0}}{\phi_{n_0}}$ represents relative volumetric fraction at z = 0. By considering mean value of Eq.(23) equality of ϕ_b, in each section x is equal to its reference value ϕ_0, which yields

$$\int_0^1\phi_b dz=0\,. \tag{26}$$

Eq. (26) gives the value of ϕ_0 in terms of Q_1 and Q_2 as

$$\phi_0=\frac{N_A}{1-Q_3}\left(\frac{1}{e^{Q_1}-1}-\frac{Q_3}{e^{Q_2}-1}\right). \tag{27}$$

From Eq.(27) and (23), one gets

$$\phi_b=\frac{N_A}{1-Q_3}\left(\frac{e^{Q_1 z}}{e^{Q_1}-1}-\frac{Q_3 e^{Q_2 z}}{e^{Q_2}-1}\right). \tag{28}$$

where: $Q_3=\dfrac{Q_2}{Q_1}$.

PERTURBATION EQUATIONS

Now we shall explore at the hypothesis of a frozen profile. We write t_0 for t in the basic solution Eqs.(22) and (28) and

$$Q_1=U(1+\tau\cos\omega t_0)\ \text{ and }\ Q_2=\frac{Q_1L_e}{\varepsilon_n}\,. \tag{29}$$

Since our interest is to examine the stability pertaining to basic state, therefore, infinitely small disturbances are superimposed to the basic state of involved physical variables as

$$\overrightarrow{q_n}=\overrightarrow{q_b}+\overrightarrow{q'}\,,\ P=P_b+P'\,,\ J_z=J_{zb}+J'\,,\ T=T_b+T'\,,$$

$$\gamma_n=\gamma_b+\gamma'\,,\ \overrightarrow{E_n}=\overrightarrow{E_b}+\overrightarrow{E'}\,,\ \phi_n=\phi_b+\phi'\,,\ \varphi_n=\varphi_b+\varphi'\,, \tag{30}$$

where perturbed quantities are denoted by primes. Using Eq.(30) in Eqs.(12)-(18) satisfying the basic state solutions Eq.(20) and applying linear stability analysis, the linearized non-dimensional equations (neglecting asterisk for simplicity) for small perturbations are

$$\left(\nabla^2+T_a\frac{\partial^2}{\partial z^2}\right)w=\left[R_e\nabla_H^2\left(T-\frac{\partial\varphi}{\partial z}\right)+R_a\nabla_H^2T-R_N\nabla_H^2\phi\right], \tag{31}$$

$$\frac{\partial T}{\partial t}+\vec{q}.\nabla T_b+\overrightarrow{q_b}.\nabla T=\nabla^2 T\,, \tag{32}$$

$$\frac{1}{\sigma}\frac{\partial\phi}{\partial t}+\frac{1}{\varepsilon_n}(\vec{q}.\nabla\phi_b+\overrightarrow{q_b}.\nabla\phi)=\frac{1}{L_e}\nabla^2\phi+\frac{N_A}{L_e}\nabla^2 T\,, \tag{33}$$

$$\nabla^2\varphi-\frac{\partial T}{\partial z}=0\,, \tag{34}$$

$$\gamma=-eT\Delta T\,, \tag{35}$$

$$J_z=-\left(\frac{\partial\phi}{\partial z}+N_A\frac{\partial T}{\partial z}\right). \tag{36}$$

LINEAR STABILITY ANALYSIS

Since the linear eigenvalue set of Eqs.(31)-(34) comprise of constant coefficients, therefore, a general solution varying exponentially on z is possible. We use normal mode technique, in which each arbitrary disturbance of dependent variable is analysed in terms of normal modes, as well as to assess stability of individual modes, as

$$[w,T,\phi,\varphi]=[W(z),\Theta(z),\Phi(z),\Psi(z)]e^{i(l_x x+l_y y)+\varpi t}, \quad (37)$$

where: $\varpi = \omega_r + i\omega_i$ is the growth rate of disturbance; l_x and l_y are horizontal wave numbers; $a = (l_x^2 + l_y^2)^{1/2}$ is resultant wave number of the disturbance.

Using Eq.(37) in Eqs.(31)-(34) and after some simplifications, the obtained stability equations are as under

$$(D^2-a^2+T_aD^2)W=\left[-(R_ea^2+R_aa^2)\Theta+R_Na^2\Phi+R_ea^2D\Psi\right], \quad (38)$$

$$-\frac{dT_b}{dz}W+(D^2-a^2-\varpi-Q_1D)\Theta=0, \quad (39)$$

$$-\frac{1}{\varepsilon_n}\frac{d\phi_b}{dz}W+\frac{N_A}{L_e}(D^2-a^2)\Theta+\left[\frac{(D^2-a^2)}{L_e}-\frac{\varpi}{\sigma}-\frac{Q_1}{\varepsilon_n}D\right]\Phi=0, \quad (40)$$

$$(D^2-a^2)\Psi-D\Theta=0. \quad (41)$$

The boundary conditions Eq.(19) in view of Eq.(37) transform to

$$W = D^2W = 0,\ \Theta = 0,\ D\Psi = 0,\ D\Phi + N_AD\Theta = 0 \quad \text{at} \quad z = 0 \quad \text{and} \quad z = 1. \quad (42)$$

METHOD OF SOLUTIONS (EXACT SOLUTION)

The Eqs.(38)-(41) with boundary conditions Eq.(42) for the stress-free bounding surfaces constitute a characteristic equation with characteristic R_a whose solutions ought to be obtained. Therefore, the appropriate solutions of lowest mode satisfying the boundary conditions Eq.(42) are taken as

$$W=A_1\sin\pi z,\ \Theta=B_1\sin\pi z,\ \Phi=-C_1N_A\sin\pi z, \quad \text{and} \quad \Psi=D_1\cos\pi z. \quad (43)$$

Using this solution in Eqs.(38)-(41) and the condition of orthogonality over the range of z satisfying the boundary condition Eq.(42), we get the matrix form as

$$\begin{bmatrix} -(J_1+\pi^2T_a) & a^2(R_e+R_a) & N_AR_Na^2 & \pi^2a^2R_e \\ \frac{4\pi^2}{4\pi^2+Q_1^2} & -J_1-\varpi & 0 & 0 \\ J_2N_A^2 & \frac{N_A^2J_1}{L_e} & -N_A^2\left(\frac{J_1}{L_e}+\frac{\varpi}{\sigma}\right) & 0 \\ 0 & -\pi & 0 & -J_1 \end{bmatrix}\begin{bmatrix} A_1 \\ B_1 \\ C_1 \\ D_1 \end{bmatrix}=0 \quad (44)$$

where: $J_1 = (a^2 + \pi^2)$; $J_2=\frac{4\pi^2(4\pi^2\varepsilon_n-L_eQ_1^2)}{(4\pi^2+Q_1^2)(4\pi^2\varepsilon_n^2+L_e^2Q_1^2)}$.

The vanishing of coefficient matrix in Eq.(44) for occurrence of a non-trivial solution yields the thermal Rayleigh number R_a as

$$R_a=-R_e\frac{a^2}{(a^2+\pi^2)}+\frac{(4\pi^2+Q_1^2)\left[(a^2+\pi^2+\varpi)\{a^2+\pi^2(1+T_a)\}\right]}{4a^2\pi^2}+$$
$$+\sigma\frac{N_A\left[4\pi^2(a^2+\pi^2)(\varepsilon_n^2+1)+\varpi(4\pi^2\varepsilon_nL_e-L_e^2Q_1^2)\right]R_N}{(4\pi^2\varepsilon_n^2+L_e^2Q_1^2)\left[(a^2+\pi^2)\sigma+\varpi L_e\right]}, \quad (45)$$

which gives on putting $\varpi = i\omega_i \neq 0$ for pure oscillatory convection, and after simplifications

$$R_a=\Delta_1+i\omega_i\Delta_2, \quad (46)$$

where,

$$\Delta_1=\frac{(a^2+\pi^2)(4\pi^2+Q_1^2)}{4\pi^2a^2}[a^2+\pi^2(1+T_a)]-R_e\frac{a^2}{(a^2+\pi^2)}-$$
$$-\sigma R_NN_A\frac{L_e^2\omega_i^2(4\pi^2\varepsilon_n-L_eQ_1^2)}{(4\pi^2\varepsilon_n^2+L_e^2Q_1^2)[L_e^2\omega_i^2+(a^2+\pi^2)^2\sigma^2]}-$$
$$-\sigma R_NN_A\frac{(a^2+\pi^2)^2[4\pi^2(L_e+\varepsilon_n)\varepsilon_n\sigma]}{(4\pi^2\varepsilon_n^2+L_e^2Q_1^2)[L_e^2\omega_i^2+(a^2+\pi^2)^2\sigma^2]}, \quad (47)$$

$$\Delta_2=\frac{(4\pi^2+Q_1^2)[a^2+\pi^2(1+T_a)]}{4\pi^2a^2}+$$
$$+R_NL_eN_A\sigma\frac{(a^2+\pi^2)[4\pi^2(-\sigma+\varepsilon_n+L_e)\varepsilon_n+\sigma L_eQ_1^2]}{(4\pi^2\varepsilon_n^2+L_e^2Q_1^2)[L_e^2\omega_i^2+(a^2+\pi^2)^2\sigma^2]}. \quad (48)$$

MATHEMATICAL ANALYSIS

Stationary convection

The occurrence of stationary modes is described by taking $\omega_i = 0$ in Eq.(47) which yields the thermal Rayleigh number of stationary modes

$$R_a^s=\frac{(\pi^2+a^2)(a^2+\pi^2+\pi^2T_a)(4\pi^2+Q_1^2)}{4\pi^2a^2}-$$
$$-R_e\frac{a^2}{(a^2+\pi^2)}-\frac{N_AR_N\left[4\pi^2(L_e+\varepsilon_n)\varepsilon_n\right]}{(4\pi^2\varepsilon_n^2+L_e^2Q_1^2)}. \quad (49)$$

It is observed from Eq.(49) that the value of R_a remains unaffected due to sign of Q_1, the parameter accounting for pulsating throughflow on the stability. As t_0 varies, the value of Q_1^2 lies between a minimum $U^2(1 - \tau^2)$ and a maximum $U^2(1 + \tau^2)$, consequently, the physical system is stabilized large enough due to the presence of pulsating throughflow along both directions.

To examine the effects of the involved non-dimensional parameters, the pulsating throughflow Q_1, modified diffusivity ratio N_A, electric Rayleigh parameter R_e, medium porosity ε_n, Taylor number T_a, nanofluid Lewis number L_e, and Rayleigh number concentration R_N, on the stability of stationary modes, the behaviour of $\frac{\partial R_a^s}{\partial Q_1}$, $\frac{\partial R_a^s}{\partial R_n}$, $\frac{\partial R_a^s}{\partial N_A}$, $\frac{\partial R_a^s}{\partial R_e}$, $\frac{\partial R_a^s}{\partial \varepsilon_n}$, $\frac{\partial R_a^s}{\partial T_a}$, and $\frac{\partial R_a^s}{\partial L_e}$ have been examined analytically. Equation (49) yields that

$$\frac{\partial R_a^s}{\partial Q_1}=\frac{1}{2}(\pi^2+a^2)\left(\frac{1}{\pi^2}+\frac{1+T_a}{a^2}\right)Q_1+$$
$$+\frac{8\pi^2\varepsilon_n(\varepsilon_n+L_e)L_e^2R_NQ_1N_A}{(4\pi^2\varepsilon_n^2+L_e^2Q_1^2)^2}, \quad (50)$$

$$\frac{\partial R_a^s}{\partial R_N}=-\frac{4\pi^2\varepsilon_n(\varepsilon_n+L_e)N_A}{(4\pi^2\varepsilon_n^2+L_e^2Q_1^2)}, \quad (51)$$

$$\frac{\partial R_a^s}{\partial N_A}=-\frac{4\pi^2R_N\varepsilon_n(\varepsilon_n+L_e)}{(4\pi^2\varepsilon_n^2+L_e^2Q_1^2)}, \quad (52)$$

$$\frac{\partial R_a^s}{\partial R_e}=-\frac{a^2}{(a^2+\pi^2)}, \quad (53)$$

$$\frac{\partial R_a^s}{\partial \varepsilon_n}=\frac{4\pi^2L_eN_A(4\pi^2\varepsilon_n^2-2\varepsilon_nL_eQ_1^2-L_e^2Q_1^2)R_N}{4(4\pi^2\varepsilon_n^2+L_e^2Q_1^2)^2}, \quad (54)$$

$$\frac{\partial R_a^s}{\partial T_a}=\frac{(\pi^2+a^2)(4\pi^2+Q_1^2)}{4a^2}, \quad (55)$$

$$\frac{\partial R_a^s}{\partial L_e}=\frac{4\pi^2R_N\varepsilon_nN_A(-4\pi^2\varepsilon_n^2+2\varepsilon_nL_eQ_1^2+L_e^2Q_1^2)}{(4\pi^2\varepsilon_n^2+L_e^2Q_1^2)^2}. \quad (56)$$

Equations (50) and (55) depict that pulsating throughflow Q_1 and Taylor-Darcy number T_a are positive for all wavenumbers, implying thereby that pulsating throughflow and angular velocity always stabilize a physical system for all wavenumbers; whereas destabilizing effect of electric field, medium porosity ε_n, the diffusivity ratio (modified) and the concentration Darcy-Rayleigh number are assessed from Eqs.(51)-(54) for all wave numbers. The Lewis number stabilizes or destabilizes a system for $L_eQ_1^2(2\varepsilon_n + L_e) > 0$ or < 0 as is clear from Eq.(56).

Now special cases arise:

Case I: in the absence of rotation, i.e. $T_a = 0$, Eq.(49) condenses to

$$R_a^s=-R_e\frac{a^2}{(a^2+\pi^2)}+\frac{(a^2+\pi^2)^2(4\pi^2+Q_1^2)}{4\pi^2a^2}-\frac{N_AR_N[4\pi^2(L_e+\varepsilon_n)\varepsilon_n]}{(4\pi^2\varepsilon_n^2+L_e^2Q_1^2)}, \quad (57)$$

which coincides with earlier result by Yadav, /36/.

Case II: for regular fluids and absence of electric field, i.e. $L_e = R_N = N_A = 0$, $R_e = 0$, Eq.(57) further shrinks to

$$R_a^s=\frac{(a^2+\pi^2)^2(4\pi^2+Q_1^2)}{4\pi^2a^2}-\frac{N_AR_N[4\pi^2(L_e+\varepsilon_n)\varepsilon_n]}{(4\pi^2\varepsilon_n^2+L_e^2Q_1^2)}. \quad (58)$$

This result agrees well with the result by Yadav, /42/.

Case III: in non-pulsating throughflow, i.e. $Q_1 = 0$, the Eq.(58) further reduces to

$$R_a^s=\frac{(a^2+\pi^2)^2}{a^2}, \quad (59)$$

which is the well-known result for regular fluids in porous medium.

CONVECTION OF OSCILLATORY MODES

Comparing real and imaginary part of Eq.(46), the value of thermal Rayleigh number of oscillatory modes is given as

$$R_a^{osc}=-R_e\frac{a^2}{(a^2+\pi^2)}+\frac{(a^2+\pi^2)(4\pi^2+Q_1^2)[a^2+\pi^2(1+T_a)]}{4\pi^2a^2}-R_NN_A\sigma\frac{L_e^2\omega_i^2(4\pi^2\varepsilon_n-L_eQ_1^2)+(\pi^2+a^2)^2\{4\pi^2(L_e+\varepsilon_n)\varepsilon_n\sigma\}}{(4\pi^2\varepsilon_n^2+L_e^2Q_1^2)[L_e^2\omega_i^2+(a^2+\pi^2)^2\sigma^2]} \quad (60)$$

and the frequency of oscillatory modes is expressed by the following expression

$$\omega_i^2=-\frac{(a^2+\pi^2)\sigma^2}{L_e^2}-\frac{16\pi^4a^2\sigma N_AR_N\varepsilon_n}{[a^2+\pi^2(1+T_a)](4\pi^2+Q_1^2)(4\pi^2\varepsilon_n^2+L_e^2Q_1^2)}+\frac{4\pi^2a^2\sigma L_eN_AR_N[4\pi^2(\sigma-\varepsilon_n)\varepsilon_n-\sigma Q_1^2L_e]}{L_e^2[a^2+\pi^2(1+T_a)](4\pi^2+Q_1^2)(4\pi^2\varepsilon_n^2+L_e^2Q_1^2)}. \quad (61)$$

The oscillatory neutral solution exists for at least one positive root of Eq.(61). It is noticed from Eq.(61) that oscillatory convection remains unaffected with electric field. In non-dispersion of nanoparticles ($R_N = 0$, $N_A = 0$), the frequency of oscillations becomes $\omega_i^2=-\frac{(a^2+\pi^2)\sigma^2}{L_e^2}<0$. Hence, the oscillatory convection does not occur for regular fluid with pulsating throughflow and rotation.

Using values of the non-dimensional parameters pertaining to nanoparticles by Buongiorno, /14/, Yadav /29, 36/, that of the Lewis number L_e ranges in $10^1 – 10^3$, Rayleigh number concentration R_N, diffusivity ratio (modified) N_A and σ, 1 – 10 and that of porosity ε_n, 0 – 1, it is observed from Eq.(61) that the frequency of oscillatory mode is always negative, i.e. $\omega_i^2 < 0$. Consequently, there is no real positive root which is necessary for the onset of oscillatory convection. Hence, the oscillatory motions do not occur for realistic boundary conditions.

NUMERICAL RESULTS AND DISCUSSION

The expression of non-oscillatory thermal Rayleigh number, the deciding parameter of stability, is encapsulated in Eq.(49) to examine the impact of pertinent non-dimensional parameters on the stability of a system. The values of these thermal Rayleigh numbers with variations in wave number are computed numerically using MATHEMATICA-12® by varying one of the non-dimensional parameters keeping other fixed with permissible values taken by many authors Buongiorno /14/, Yadav /36/, and Yadav et al. /43/, many more, i.e. $R_n = 0.5$, $N_A = 3$, $L_e = 20$, $R_e = 10$, $Q_1 = 0.8$, $T_a = 5$, $\varepsilon_n = 0.5$. These numerically computed results have been represented graphically in Figs. 2-8 for both top- heavy as well as bottom heavy arrangements of nanoparticles.

The variation of electric Rayleigh number, R_e, accounting for AC electric field against the wave number is displayed in Fig. 2. It is assessed from figures that value of thermal Rayleigh number falls with rise in electric Rayleigh number, thereby advancing the initiation of stationary convection. It is also assessed that the critical wave number attains the same value i.e., however, the corresponding critical thermal Rayleigh number falls. Thus, the stability region under stationary modes is shrunk. This happens so for; the stability of the system is lowered with increasing the strength of the electric field and electrostatic energy. However, the critical wavenumber remains unaffected.

The effect of various values of Lewis number, L_e, on the thermal Rayleigh number versus a on the neutral curves is assessed in Fig. 3. It is depicted that a rise in the thermal Rayleigh number is observed with an increment in L_e. This rise occurs due to the increase in Brownian motion of the nanoparticles with an increment in L_e. However, the critical wavenumber remains unaffected.

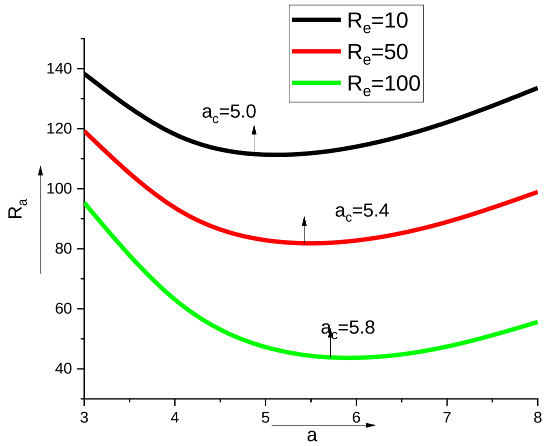

R_N=0.5, N_A=3, Q_1=0.8, T_a=5, R_e=10, L_e=20, ε_n=0.5.

Figure 2. Plot of neutral curves R_a against a vs. parameter R_e.

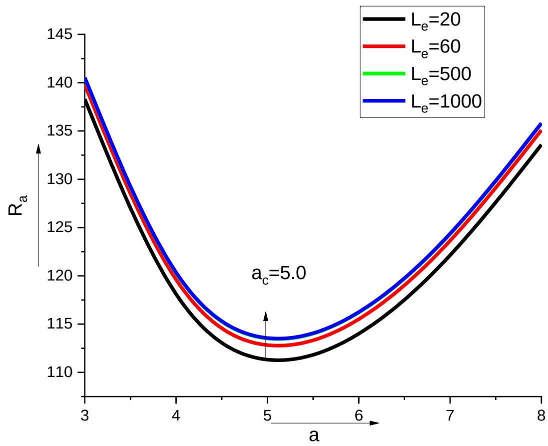

R_N=0.5, N_A=3, Q_1=0.8, T_a=5, R_e=10, L_e=20, ε_n=0.5.

Figure 3. Plot of neutral curves of R_a against a vs. parameter L_e.

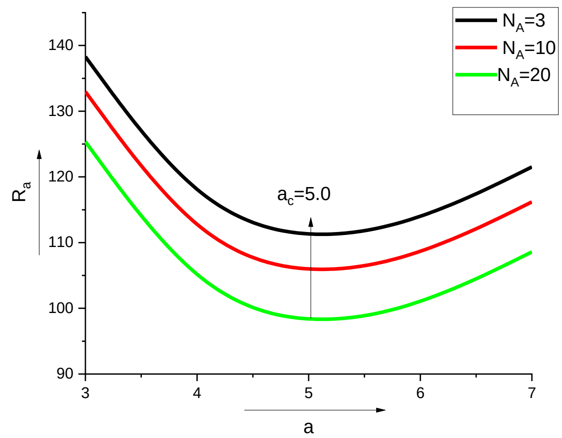

R_N=0.5, N_A=3, Q_1=0.8, T_a=5, R_e=10, L_e=20, ε_n=0.5.

Figure 4. Plot of neutral curves of R_a against a vs. parameter N_A.

The impact of modified diffusivity ratio N_A and the concentration Rayleigh number R_N on the framework of stability are displayed in Figs. 4 and 5. It is assessed from Figs. 4 and 5 that increment in the values of both Rayleigh number and modified diffusivity ratio of nanoparticles decrease the critical Rayleigh number. Consequently, both these parameters tend to advance onset of stationary modes in nanofluids. It happens so because the thermophoresis, as well as nanoparticle's Brownian rise in lieu of increasing values of both Rayleigh number and modified diffusivity ratio of the nanoparticles. It is also illustrated from the figures that the critical wave number remains unaffected.

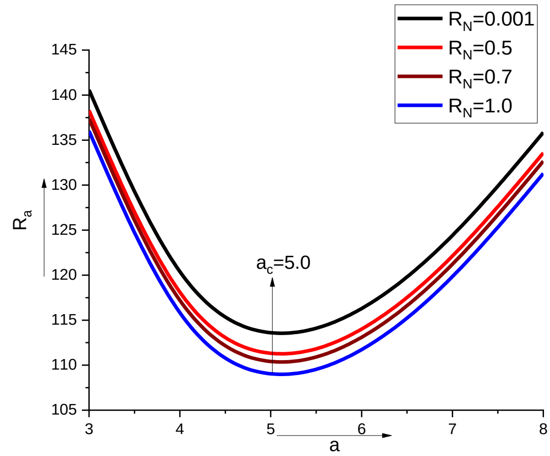

R_N=0.5, N_A=3, Q_1=0.8, T_a=5, R_e=10, L_e=20, ε_n=0.5.

Figure 5. Plot of neutral curves of R_a against a vs. parameter R_N.

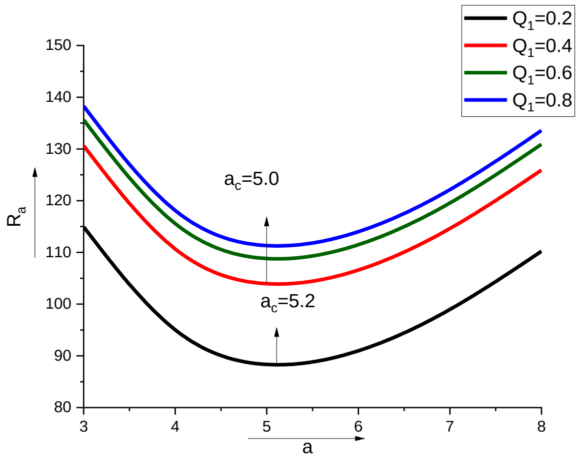

R_N=0.5, N_A=3, Q_1=0.8, T_a=5, R_e=10, L_e=20, ε_n=0.5.

Figure 6. Plot of neutral curves of R_a against a vs. parameter Q_1.

The impact of distinct values of pulsating throughflow parameter Q_1, on the thermal Rayleigh number versus wave number a is shown in Fig. 6. It is depicted that the thermal Rayleigh number takes higher values with an increment in the pulsating throughflow parameter, thereby shrinking the size of convection cells and expanding the region of stability. A fall in the critical wave number with rise in the pulsating throughflow parameter is also observed. Thus, the system is stabilized large enough with pulsating throughflow parameter.

Figure 7 reveals that the thermal Rayleigh number decreases with an increment in medium porosity ε_n. Thus, medium porosity shows a destabilizing effect on stationary convection. This happens because the volume of the solid matrix enhances with a rise in the medium porosity. It is also observed that the critical thermal Rayleigh number descends, while value of the critical wave number is unchanged.

Figure 8 demonstrates the impact of various values of the Taylor number T_a, accounting for angular velocity of the fluid on the framework of stability. It is depicted from the figure that there is an enhancement in the critical wave number and Rayleigh number with an increment in the rotation parameter. Therefore, the region of stability under the stationary modes is enhanced meaning, thereby, shrinking substantially the size of convective cells. Thus, rotation tends to suppress the fluid motion along the vertical, and the convection as well.

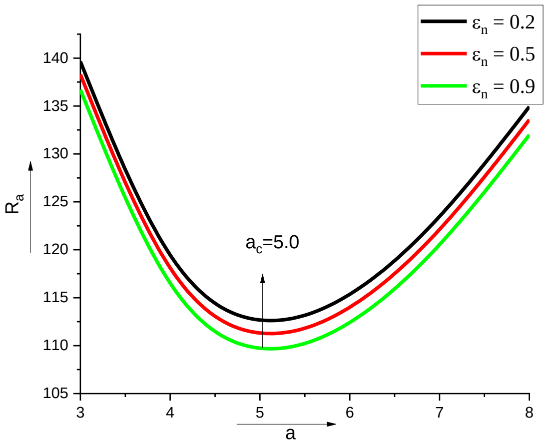

R_N=0.5, N_A=3, Q_1=0.8, T_a=5, R_e=10, L_e=20, ε_n=0.5.

Figure 7. Plot of neutral curves of R_a against a vs. parameter ε_n.

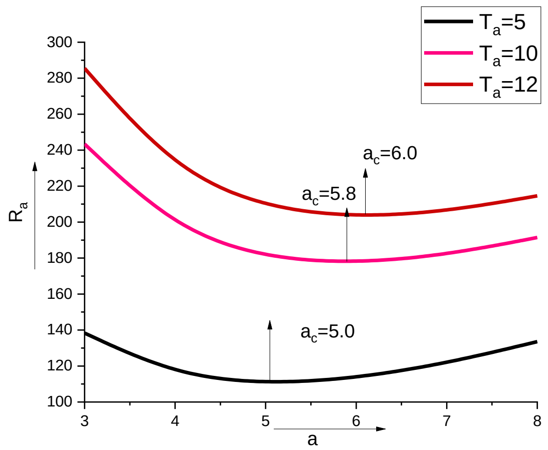

R_N=0.5, N_A=3, Q_1=0.8, T_a=5, R_e=10, L_e=20, ε_n = 0.5.

Figure 8. Plot of neutral curves of R_a against a vs. parameter T_a.

CONCLUSIONS

The joint effect of vertical electric field and pulsating throughflow on the occurrence of thermal convection in a nanofluid layer rotating about the vertical in a porous media by employing Darcy law is examined analytically for realistic stress-free boundary conditions. The Boungiorno model integrates effects of Brownian motion and thermophoresis diffusion coefficients with that of electrophoresis and electrostatic energy. The stability criterion is analysed by applying linear theory, normal mode technique and one term Galerkin approximation. The numerically computed values of the thermal Rayleigh number with respect to pertinent involved parameters individually on the onset of stationary modes are represented graphically. It is established that pulsating throughflow and rotation tend to stabilize a system substantially. A system is destabilised by the electric field, modified diffusive ratio, and nanoparticle Rayleigh number. The Lewis number and the medium porosity stabilize or destabilize a system under certain conditions involving parameters.

ACKNOWLEDGEMENT

Authors would like to thank the editor for the necessary corrections and formatting of the paper.

REFERENCES

1. Gross, M.J., Porter, J.E. (1966), *Electrically induced convection in dielectric liquids*, Nature, 212: 1343-1345. doi: 10.1038/212 1343a0
2. Turnbull, R.J. (1969), *Effect of dielectrophoretic forces on the Bénard instability*, The Phys. Fluids, 12(9): 1809-1815. doi: 10 .1063/1.1692745
3. Wang, C.Y. (1971), *Pulsatile flow in a porous channel*, J Appl. Mech. 38(2): 553-555. doi: 10.1115/1.3408822
4. Ishino, Y., Suzuki, M., Abe, T., et al. (1996), *Flow and heat transfer characteristics in pulsating pipe flows (effects of pulsation on internal heat transfer in a circular pipe flow)*, Heat Transfer-Jap. Res. 25(5): 323-341. doi: 10.1002/(SICI)1520-65 56(1996)25:5<323::AID-HTJ5>3.0.CO;2-Z
5. Choi, S.U.S., Eastman, J.A. (1995), *Enhancing thermal conductivity of fluids with nanoparticles*, In: D.A. Siginer, H.P. Wang (Eds.), Developments and Applications of Non-Newtonian Flows, ASME, New York, 66: 99-105.
6. Keblinski, P., Eastman, J.A., Cahill, D.G. (2005), *Nanofluids for thermal transport*, Mater. Today, 8(6): 36-44. doi: 10.1016/ S1369-7021(05)70936-6
7. Choi, S.U.S., Zhang, Z.G., Yu, W., et al. (2001), *Anomalous thermal conductivity enhancement in nanotube suspensions*, Appl. Phys. Lett. 79(14): 2252-2254. doi: 10.1063/1.1408272
8. Wang, X., Xu, X., Choi, S.U.S. (1999), *Thermal conductivity of nanoparticle - fluid mixture*, J Thermophys. Heat Transf. 13 (4): 474-480. doi: 10.2514/2.6486
9. Anoop, K.B., Sundararajan, T., Das, S.K. (2009), *Effect of particle size on the convective heat transfer in nanofluid in the developing region*, Int. J Heat Mass Transf. 52(9-10): 2189-2195. doi: 10.1016/j.ijheatmasstransfer.2007.11.063
10. Saidur, R., Leong, K.Y., Mohammad, H.A. (2011), *A review on applications and challenges of nanofluids*, Renew. Sustain. Ener. Rev. 15(3): 1646-1668. doi: 10.1016/j.rser.2010.11.035
11. Wong, K.V., De Leon, O. (2010), *Applications of nanofluids: current and future*, Adv. Mech. Eng. 2: 1-11. doi: 10.1155/201 0/519659
12. Mahajan, A., Sharma, M.K. (2019), *Penetrative convection due to absorption of radiation in a magnetic nanofluid saturated porous layer*, Studia Geotechnica et Mechanica, 41(3): 129-142.
13. Wang, X.Q., Mujumdar, A.S. (2007), *Heat transfer characteristics of nanofluids: a review*, Int. J Therm. Sci. 46(1): 1-19. doi: 10.1016/j.ijthermalsci.2006.06.010
14. Buongiorno, J. (2006), *Convective transport in nanofluids*, J Heat Transf. 128(3): 240-250. doi: 10.1115/1.2150834
15. Nield, D.A., Kuznetsov, A.V. (2009), *Thermal instability in a porous medium layer saturated by a nanofluid*, Int. J Heat Mass Transf. 52(25-26): 5796-5801. doi: 10.1016/j.ijheatmasstransfe r.2009.07.023
16. Dhananjay, Y., Agrawal, G.S., Bhargava, R. (2011), *Rayleigh-Bénard convection in nanofluid*, Int. J Appl. Math. Mech. 7(2): 61-76.
17. Xu, H., Xing, Z. (2017), *The lattice Boltzmann modeling on the nanofluid natural convective transport in a cavity filled with a porous foam*, Int. Comm. Heat Mass Transf. 89: 73-82. doi: 10. 1016/j.icheatmasstransfer.2017.09.013
18. Riahi, D.N. (2005), *Flow instabilities in a horizontal dendrite layer rotating about an inclined axis*, J Porous Media, 8(3): 327- 342. doi: 10.1615/JPorMedia.v8.i3.70

19. Bhadauria, B.S. (2007), *Fluid convection in a rotating porous layer under modulated temperature on the boundaries*, Transp. Porous Med. 67: 297-315. doi: 10.1007/s11242-006-9027-x
20. Bhadauria, B.S. (2008), *Effect of temperature modulation on the onset of Darcy convection in a rotating porous medium*, J Porous Med. 11(4): 361-375. doi: 10.1615/JPorMedia.v11.i4.30
21. Vadasz, P. (2019), *Instability and convection in rotating porous media: A review*, Fluids, 4(3): 147. doi: 10.3390/fluids4030147
22. Chand, R., Rana, G.C. (2012), *On the onset of thermal convection in rotating nanofluid layer saturating a Darcy-Brinkman porous medium*, Int. J Heat Mass Transf. 55(21-22): 5417-5424. doi: 10.1016/j.ijheatmasstransfer.2012.04.043
23. Vanishree, R.K., Siddheshwar, P.G. (2010), *Effect of rotation on thermal convection in an anisotropic porous medium with temperature-dependent viscosity*, Transp. Porous Med. 81: 73-87. doi: 10.1007/s11242-009-9385-2
24. Shivakumara, I.S., Ng, C.-O., Nagashree, M.S. (2011), *The onset of electrothermoconvection in a rotating Brinkman porous layer*, Int. J Eng. Sci. 49(7): 646-663. doi: 10.1016/j.ijengsci.20 11.02.010
25. Yadav, D., Agrawal, G.S., Lee, J. (2016), *Thermal instability in a rotating nanofluid layer: A revised model*, Ain Shams Eng. J, 7(1): 431-440. doi: 10.1016/j.asej.2015.05.005
26. Bakar, N.A.A., Bachok, N., Arifin, N.M. (2017), *Rotating flow over a shrinking sheet in nanofluid using Buongiorno model and thermophysical properties of nanoliquids*, J Nanofluids, 6(6): 1215-1226. doi: 10.1166/jon.2017.1414
27. Yadav, D. (2020), *Effects of rotation and varying gravity on the onset of convection in a porous medium layer: a numerical study*, World J Eng. 17(6): 785-793. doi: 10.1108/WJE-03-202 0-0086
28. Zhakin, A.I. (2012), *Electrohydrodynamics*, Physics-Uspekhi, 55(5): 465. doi: 10.3367/UFNe.0182.201205b.0495
29. Yadav, D., Lee, J., Cho, H.H. (2016), *Electrothermal instability in a porous medium layer saturated by a dielectric nanofluid*, J Appl. Fluid Mech. 9(5): 2123-2132. doi: 10.18869/ACADPUB .JAFM.68.236.25140
30. Chand, R., Rana, G.C. (2016), *Electrothermo convection of rotating nanofluid in Brinkman porous medium*, Spec. Topics Rev. Porous Med.: Int. J, 7(2): 181-194.
31. Sharma, V., Kumar, A., Abhilasha, Sharma, A. (2017), *Numerical investigations of electro-thermal convection in dielectric nanofluid layer*, Res. J Sci. Technol. 9(1): 184-188. doi: 10.595 8/2349-2988.2017.00031.6
32. Rana, G.C., Saxena, H., Gautam, P.K. (2019), *The onset of electrohydrodynamic instability in a couple-stress nanofluid saturating a porous medium: Brinkman model*, Rev. Cubana de Fisica, 36(1): 37-45.
33. Rana, G.C., Saxena, H., Gautam, P.K. (2019), *Electrohydrodynamic thermal instability in a porous medium layer saturated by a Walters' (model B') elastico-viscous nanofluid*, Struct. Integ. and Life, 19(2): 86-93.
34. Rana, G.C., Gautam, P.K., Saxena, H. (2019), *Electrohydrodynamic thermal instability in a Walters' (model B') rotating nanofluid saturating a porous medium*, J the Serb. Soc. Comp. Mech. 13(2): 19-35. doi: 10.24874/jsscm.2019.13.02.03
35. Rana, G.C., Gautam, P.K., Saxena, H. (2021), *Oscillatory motions in an electrothermal-convection in shear-thinning visco-elastic nanofluid layer in a porous medium*, Struct. Integ. and Life, 21(1): 108-117.
36. Gautam, P.K., Rana, G.C., Saxena, H. (2020), *Stationary convection in the electrohydrodynamic thermal instability of Jeffrey nanofluid layer saturating a porous medium: free-free, rigid-free, and rigid-rigid boundary conditions*, J Porous Med. 23 (11): 1043-1063. doi: 10.1615/JPorMedia.2020035061
37. Yadav, D. (2018), *The influence of pulsating throughflow on the onset of electro-thermo-convection in a horizontal porous medium saturated by a dielectric nanofluid*, J Appl. Fluid Mech. 11(6): 1679-1689.
38. Abbasian Arani, A.A., Jahani, A. (2020), *Turbulent pulsating nanofluids flow and heat transfer inside constant heat flux boundary condition helical-coil tube*, AUT J Mech. Eng. 4(3): 289-300. doi: 10.22060/AJME.2019.16137.5807
39. Saini, S., Sharma, Y.D. (2017), *The effect of vertical throughflow in Rivlin-Ericksen elastico-viscous nanofluid in a non-Darcy porous medium*, Nanosyst.: Phys., Chem., Math. 8(5): 606-612. doi: 10.17586/2220-8054-2017-8-5-606-612
40. Zahmatkesh, I., Naghedifar, S.A. (2018), *Pulsating nanofluid jet impingement onto a partially heated surface immersed in a porous layer*, Jordan J Mech. Indust. Eng. 12(2): 99-107.
41. Yadav, D. (2019), *The effect of pulsating throughflow on the onset of magneto convection in a layer of nanofluid confined within a Hele-Shaw cell*, Proc. Institut. Mech. Eng. Part E: J Proc. Mech. Eng. 233(5): 1074-1085. doi: 10.1177/095440891 9836362
42. Yadav, D. (2021), *The effect of rotation and pulsating throughflow on the onset of longitudinal convective rolls in a porous medium saturated by nanofluid*, J Porous Med. 24(10): 49-63. doi: 10.1615/JPorMedia.2021026073
43. Yadav, D., Mohamad, A.M., Rana, G.C. (2021), *Effect of throughflow on the convective instabilities in an anisotropic porous medium layer with inconstant gravity*, J Appl. Comput. Mech. 7(4): 1964-1972. doi: 10.22055/JACM.2020.32381.2006
44. Vijayalakshmi, A., Srinivas, S., Badeti, S., Subramanyam Reddy, A. (2019), *Hydromagnetic pulsating flow of nanofluid between two parallel walls with porous medium*, Mater. Today, Proc. 9(2): 306-319. doi: 10.1016/j.matpr.2019.02.161
45. Somasundaram, R., Subramanyam Reddy, A. (2021), *Pulsating flow of electrically conducting couple stress nanofluid in a channel with ohmic dissipation and thermal radiation - Dynamics of blood*, In: Proc. Institut. Mech. Eng., Part E: J Proc. Mech. Eng. 235(6): 1895-1909. doi: 10.1177/09544089211025177